Analysis of Data from Salt Reconsolidation Experiments at Sandia National Laboratories in FY12 and FY13

Fuel Cycle Research & Development

APPENDIX E

FCT DOCUMENT COVER SHEET [1]

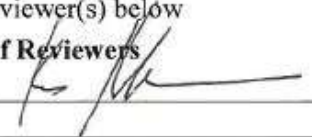| Name/Title of Deliverable/Milestone/Revision No.	Analysis of Data from Salt Reconsolidation Experiments at Sandia National Laboratories in FY12 and FY13
Work Package Title and Number	DR Salt R&D – SNL, FT-14SN081801 Rev 2
Work Package WBS Number	1.02.08.18
Responsible Work Package Manager	Christi Leigh _____ (Name/Signature)
Date Submitted	

Quality Rigor Level for Deliverable/Milestone[2]	☒ QRL-3	☐ QRL-2	☐ QRL-1 Nuclear Data	☐ Lab/Participant QA Program (no additional FCT QA requirements)

This deliverable was prepared in accordance with   Sandia National Laboratories
                                                                                    (Participant/National Laboratory Name)

QA program which meets the requirements of

☐ DOE Order 414.1   ☐ NQA-1-2000   ☐ Other

This Deliverable was subjected to:

☒ Technical Review	☐ Peer Review
Technical Review (TR)	**Peer Review (PR)**
Review Documentation Provided	**Review Documentation Provided**
☐ Signed TR Report or,	☐ Signed PR Report or,
☐ Signed TR Concurrence Sheet or,	☐ Signed PR Concurrence Sheet or,
☒ Signature of TR Reviewer(s) below	☐ Signature of PR Reviewer(s) below

Name and Signature of Reviewers

KRIS KUHLMAN

NOTE 1: *Appendix E should be filled out and submitted with the deliverable. Or, if the PICS:NE system permits, completely enter all applicable information in the PICS:NE Deliverable Form. The requirement is to ensure that all applicable information is entered either in the PICS:NE system or by using the FCT Document Cover Sheet.*

NOTE 2: *In some cases there may be a milestone where an item is being fabricated, maintenance is being performed on a facility, or a document is being issued through a formal document control process where it specifically calls out a formal review of the document. In these cases, documentation (e.g., inspection report, maintenance request, work planning package documentation or the documented review of the issued document through the document control process) of the completion of the activity, along with the Document Cover Sheet, is sufficient to demonstrate achieving the milestone. If QRL 1, 2, or 3 is not assigned, then the Lab / Participant QA Program (no additional FCT QA requirements) box must be checked, and the work is understood to be performed and any deliverable developed in conformance with the respective National Laboratory / Participant, DOE or NNSA-approved QA Program.*

Sandia
National
Laboratories

SUMMARY

Design, analysis and performance assessment of potential salt repositories for heat-generating nuclear waste require knowledge of thermal, mechanical, and fluid transport properties of reconsolidating granular salt. To inform salt repository evaluations, we have undertaken an experimental program to determine Bulk and Young's moduli and Poisson's ratio of reconsolidated granular salt as a function of porosity and temperature and to establish the deformational processes by which the salt reconsolidates. Tests were conducted at 100°, 175° or 250°C. In hydrostatic tests, confining pressure is increased to 20 MPa with periodic unload/reload loops to determine K. Volume strain increases with increasing temperature. In shear tests at 2.5 and 5 MPa confining pressure, after confining pressure is applied, the crushed salt is subjected to a differential stress, with periodic unload/reload loops to determine E and v. At predetermined differential stress levels the stress is held constant and the salt consolidates. Displacement gages mounted on the samples show little lateral deformation until the samples reach a porosity of ~10%. Interestingly, vapor is vented only for 250°C tests and condenses at the vent port. It is hypothesized the brine originates from fluid inclusions, which were made accessible by heating and intragranular deformational processes including decrepitation

CONTENTS

FIGURES

TABLES

ANALYSIS OF DATA FROM SALT RECONSOLIDATION EXPERIMENTS AT SANDIA NATIONAL LABORATORIES IN FY12 AND FY13

1.   INTRODUCTION

Understanding and predicting the reconsolidation behavior of granular crushed salt is vital to backfilling or sealing nuclear waste repositories in salt. Significant research efforts have attempted to address this recognized need resulting in a long history of crushed salt backfill testing for salt repository applications. Callahan (1999) summarized the constitutive model for room temperature consolidation with application to the shaft seal system at the Waste Isolation Pilot Plant (WIPP). Over the years, salt reconsolidation has been a topic of great interest to international salt repository studies as exemplified by recurring symposia (for example: Aubertin and Hardy, 1996 and Wallner et al., 2007). A preponderance of these studies focused on room temperature experiments, with only a few tests conducted at elevated temperatures up to 100˚C. Today there is a renewed national and international interest in salt reconsolidation at elevated temperature, particularly as applied to disposal of heat-generating nuclear waste.

In recognition of the need for this essential research, the United States (US) Department of Energy supported investigations to explore and solidify our understanding of reconsolidation of granular salt under high temperatures. For this purpose, a new experimental procedure for a laboratory study of reconsolidation of salt aggregate was developed, emphasizing testing at elevated temperature. Successful completion of these experiments under challenging pressure and temperature regimes required development of advanced geomechanics techniques.

The salt used in these experiments is called "run-of-mine" which means the aggregate was produced during normal mining operations at WIPP (with aggregate pieces greater than 9.5 mm removed). The laboratory studies provide data representing consolidation behavior as a function of stress state and temperatures up to 250˚C.

The laboratory test procedures used both hydrostatic (isostatic) and shear stresses to consolidate the mine-run salt. Hydrostatic refers to the application of a uniform or isotropic stress state, while shear stresses involve the superposition of an additional axial stress. Consolidation under shear stress more realistically represents conditions expected in a disposal concept where the roof-to-floor closure would be faster than the rib-to-rib closure.

In addition to elevated temperature, hydrostatic pressures up to 20 megapascal (MPa) and stress differences up to 10 MPa were applied. The stresses correspond to in situ stresses encountered at commercial salt mining operations as well as WIPP.

It was initially thought the effective pressure-solution redeposition process would be minimized because available and accessible brine would be driven off by high temperatures and venting of the samples. Further, it was hypothesized the intragranular fluid inclusions within the crystal structure would remain trapped. As will be discussed later in this report, neither hypothesis proved correct, which is a key finding of this research. Drying may occur with an accompanying change of consolidation mechanisms; this is a potentially important hypothesis relevant to crushed salt in a heat-generating salt repository. Such experimental work was identified to be of great interest to national and international salt repository programs (Hansen and Leigh, 2011).

2.   BACKGROUND AND TECHNIQUES

A suite of experiments was designed to systematically evaluate the consolidation of crushed salt as a function of stress (σ) and temperature (T) conditions. Laboratory studies provide consolidation behavior for temperature to 250˚C and stress to 20 MPa.

The test matrix is summarized in Table 1, which lists the test type, stress, temperature conditions, and other test information. Three test types used in this test series are isostatic, shear and shear in combination with creep of right circular cylindrical specimens. Most of the tests had multiple stages, for example, an initial isostatic segment followed by one or more shear and creep consolidation portions. The sequence and type of experimental test conditions of temperature, pressure, and shear were chosen to allow parameterization of appropriate constitutive models using a minimum number of tests.

Table 1: Test Matrix for Salt Reconsolidation at Elevated Temperature

Test Number	Test Type	T (˚C)	Isostatic Confining Pressure (MPa)	Stress Difference (MPa)
7	Isostatic	250	20.0	0.0
8/9	Isostatic/Shear	250	10.0	10.0
1/10-16	Isostatic/Shear	100	2.5	2.50/5.0
2/11-17	Isostatic/Shear	100	5.0	2.50/5.0
3/12-18	Isostatic/Shear	175	2.5	2.50/5.0
4/13-19	Isostatic/Shear	175	5.0	2.50/5.0
5/14-20	Isostatic/Shear	250	2.5	2.50/5.0
6/15-21	Isostatic/Shear	250	5.0	2.50/5.0

Table 1, cont.: Test Matrix for Salt Reconsolidation at Elevated Temperature

Test Number	Axial Stress (MPa)	Mean Stress (MPa)	Description
7	20.0	20.0	Quasistatic
8/9	20.0	13.33	Quasistatic
1/10-16	5.0/7.5	3.33/4.17	Quasistatic-Creep
2/11-17	7.5/10.0	5.83/6.67	Quasistatic-Creep
3/12-18	5.0/7.5	3.33/4.17	Quasistatic-Creep
4/13-19	7.5/10.0	5.83/6.67	Quasistatic-Creep
5/14-20	5.0/7.5	3.33/4.17	Quasistatic-Creep
6/15-21	7.5/10.0	5.83/6.67	Quasistatic-Creep

For all tests, jacketed specimens of crushed mine-run salt from the WIPP were dried at 105˚C until no further weight loss occurred. Undeformed right-circular cylindrical specimen assemblies of unconsolidated granular salt with initial porosities of ~ 40%, nominally 10 cm in diameter and 17.5 cm in length, were jacketed in malleable soldered lead tubes. Samples were placed in a pressure vessel and kept at test temperatures of 100˚, 175˚ or 250˚C and vented to the atmosphere during the entire test procedure.

In isostatic tests, confining pressure is slowly increased at pressurization rates ranging from ~ 0.0005 MPa/sec at the beginning of the test to ~0.0422 MPa/sec near the end by pumping silicon oil confining fluid at rates of 9.46 mL/min or by advancing the actuator at a rate of 0.00254 cm/sec into the pressure vessel (both pressurization methods increased pressure at equivalent but non-uniform rates). During pressurization, pressure and sample displacement (used to determine strain) are recorded. Also, at

predetermined pressure levels, pressurization is reversed to 1/3 to 1/2 the previous maximum level, then loading is resumed. This is termed an unload/reload loop; from such a loop the bulk modulus may be determined.

In shear tests, after an isostatic pressure increase to a predetermined level, the axial piston housed in the loading frame is advanced in a quasistatic manner (an actuator displacement rate of 0.00127 cm/sec is equivalent to ~8×10^{-5}/sec strain rate on a 15.49 cm long sample) until a predetermined stress level (Table 1) is attained. At predetermined axial stress levels, axial loading is reversed to 1/3 to 1/2 the starting differential stress level, then loading is resumed. In this type of unload/reload loop, the elastic Young's modulus and Poisson's ratio may be determined. The specimen is typically held at constant differential stress and allowed to creep until approximately 5% additional axial strain accrues through creep consolidation. At that point, the axial piston is advanced in a quasistatic manner until the second predetermined stress level (Table 1) is attained (accompanied by unload/reload loops during loading). The specimen is allowed to creep (and further consolidate) at the higher stress level until approximately 5% additional axial strain is experienced. Then the axial load is reduced to zero, the confining pressure is reduced to zero, and the heating elements are turned off allowing the specimen to cool to ambient temperature.

The specimen assembly (Figure 1) consists of a right circular cylinder of unconsolidated granular salt, nominally 10 cm in diameter and 17.5 cm in length, constrained vertically between specially machined aluminum end caps. The machining of the outer diameter of the end caps enables a metal-metal seal of an outer lead jacket to the end cap. The upper end cap is vented to the atmosphere during the test to prevent buildup of vapor pore pressure. Beveled face plates are placed between the end caps and salt to accommodate the diameter change for the unconsolidated salt portion of the assembly and allow space for the inner lead jacket. A porous metal frit, shown in the figure as porous felt metal, is placed below the top end cap to allow fluid migration and venting across the entire specimen top surface area. The outer lead jacket, a soldered lead tube, laterally contains the entire assemble from top to bottom, and isolates the inner lead jacket and the end caps from the confining medium. The lead is highly malleable and conforms to the shape of the specimen when hydrostatic pressure is applied.
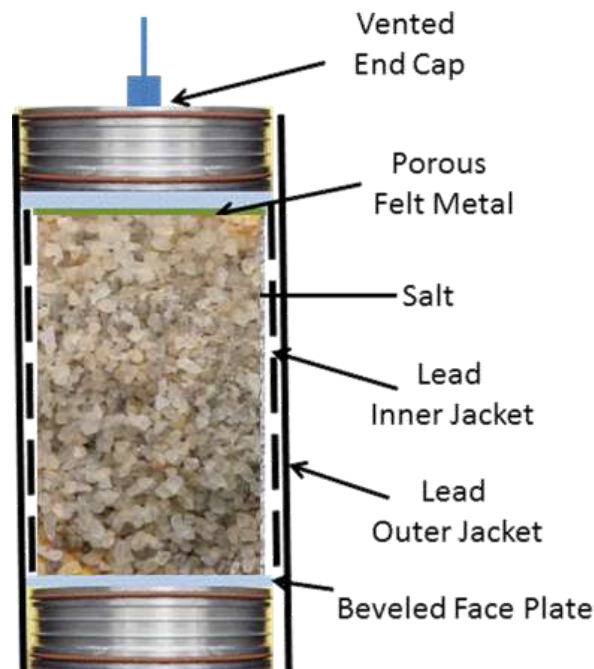

Figure 1. Schematic of Test Arrangement.

Each assembly is fitted with two high temperature lateral deformation gages (Figure 2) affixed near the specimen mid-height and oriented approximately orthogonal to one another. The specimen is placed in the pressure vessel (Figure 3) by lowering the vessel over the specimen assembly. (Figure 3 shows a specimen upon test completion below the pressure vessel.) The pressure vessel is then filled with confining fluid, heated to the test temperature at about 1˚C/min to minimize temperature gradients and allow uniform thermal expansion of the unconstrained specimen, and held at test temperature overnight at ambient pressure. At the initiation of the loading portion of the test, the isostatic pressure is increased as described above, followed by the axial force/stress being increased as described above for the shear/creep portion of the test. A reconsolidated specimen in posttest condition is shown in Figure 4. Note the significant dimpling of the lead jacket, caused by the presence of local voids and undulations in the granulated salt surface coupled with malleability of the lead jacketing material.

Figure 2. Instrumented Specimen Assembly Pretest.

Figure 3. Test Appratus with Reconsolidated Sample.

Figure 4. Specimen Post Test.

Jacket leaks were problematic at 250˚C because of extreme consolidation, large volumetric strains, and further softening of the lead jackets. To successfully mitigate the potential for jacket puncture, an intermediate thin copper sheet was placed between lead jackets for 250˚C tests as shown in Figure 5a and b.
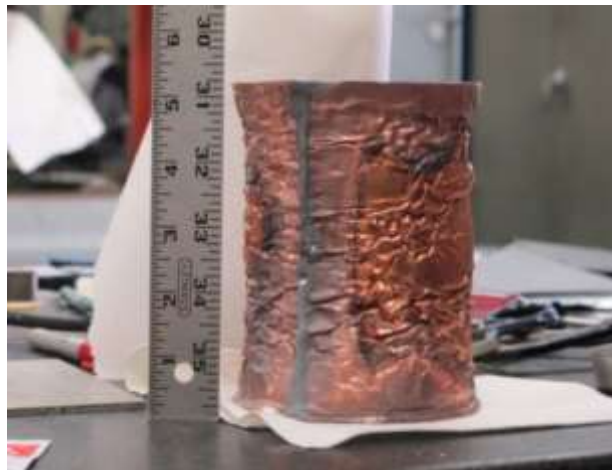
Figure 5a. Application of Copper Jacket.

Figure 5b. Copper Jacket after 250˚C test.

3.   RESULTS AND ANALYSIS

Table 2 provides a list of all laboratory tests completed and shows the correspondence of each test with the experimental matrix shown in Table 1. The experiments are numbered chronologically and identified with a unique identification number; the total volume strain, normalized density, and confining pressure are presented.

Table 2: Summary of Tests Completed

Test Number	Sample ID	Total Volumetric strain ε_V (%)	Normalized Density (% of theoretical)
2	FCT-CS-HQ-100-02	28	79
3	FCT-CS-HQ-250-01	29, Leak	78, Leak
4	FCT-CS-HQ-175-01	35	87
5	FCT-CS-HQ-175-02		
6	FCT-CS-HQ-250-02	37	93
7	FCT-CS-SQ-250-01	31, σ_C*	84, σ_C*
8	FCT-CS-SQ-250-02	37	93
9	FCT-CS-CR-250-01	33	86
10	FCT-CS-CR-250-02		
11	FCT-CS-CR-250-03		
12	FCT-CS-CR-250-04		
13	FCT-CS-CR-175-01	31	86
14	FCT-CS-CR-175-02	32	85
15	FCT-CS-CR-100-01	19	73
16	FCT-CS-CR-250-05	40	94
17	FCT-CS-CR-100-02	26	77
18	FCT-CS-CR-100-03	33	86
19	FCT-CS-CR-175-03	N/A**	N/A**
20	FCT-CS-HQ-ALL-01	39	97
21	FCT-CS-CR-ALL-02	35	90

*Values obtained after hydrostatic compaction and are not available after the shear stage.

**Data not available at this time.

Table 2, con't: Summary of Tests Completed

Test Number	Isostatic Confining pressure obtained (MPa)	Tests satisfied from test matrix (Table 1)
2	20	1,2
3	5.5	5,6
4	16.6	3,4
5		Actuator piston contacted sample at σ_C=10.3 MPa
6	20	5,6,7,8
7	10	8
8	10	9
9	2.5	14,20
10		
11		N/A (breech of confining medium into sample)
12		
13	2.5	12,18
14	5	13,19
15	2.5	10,16 (σ_D=2.5 MPa only)
16	5	15,21
17	2.5	10,16
18	5	11,17
19	2.5	12,18 (σ_D=5 MPa only)
20	20	1,2
21	20	3,4

A noteworthy, perhaps unexpected observation during these tests was the production of brine from the pore pressure port during 250°C tests (Figure 6). This occurred during the heating phase of these tests, when the specimen was unconfined.

Figure 6. Brine exiting the pore pressure port at 250˚C.

3.1   Isostatic Tests

After the test temperature had stabilized overnight, pressure was increased to 20 MPa and specimen volume change was recorded either though dilatometry or using "on specimen" gages. At all temperatures, the specimens consolidate irreversibly with increasing pressure; the compacting specimen stiffens with increasing pressure. This is clearly shown in Figure 7 where volume strain is compared to applied hydrostatic pressure for three tests at successively greater temperatures. As shown, increasing temperature facilitates compaction; i.e. more compaction is observed at a given pressure for greater temperatures. As the crushed salt is forced to compact, its normalized density increases (Figure 8). The normalized density is the calculated density during the test divided by the theoretical density of solid salt.
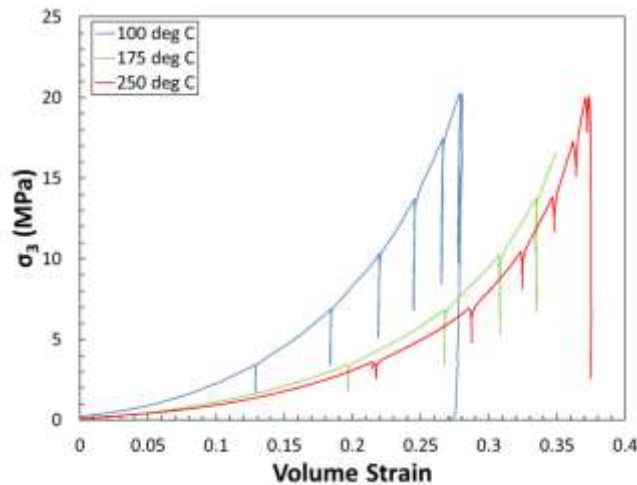

Figure 7. Volume strain versus hydrostatic confining pressure (σ_3).
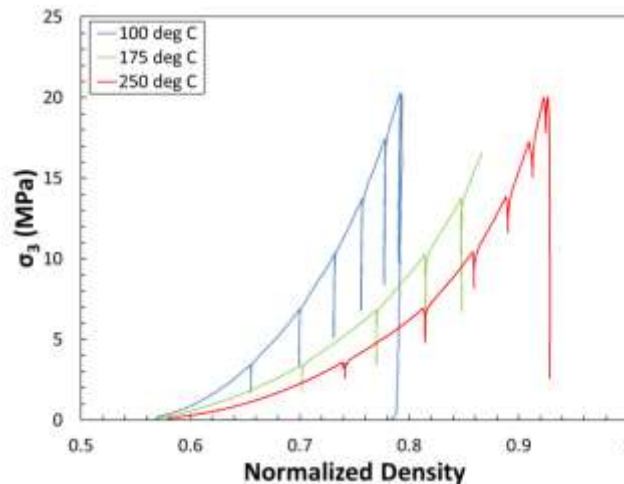
Figure 8. Normalized density versus hydrostatic confining pressure (σ_3).

The unload reload loops conducted during each test facilitate determinations of the bulk modulus (K) at intervals during the deformation. In Figure 9, K is plotted against the fractional density (the percent of theoretical density [2.165 g/cc]). K is low and insensitive to fractional density increases until a fractional density of ~75% is attained. Near this value of fractional density, K begins increasing with increasing fractional density to the maximum level observed. These data imply K is primarily dependent on fractional density and less dependent on temperature. The maximal values of K's are greater than the K of intact salt, which is a recognized and unresolved issue. The unreasonable calculated values are perhaps the result of the new experimental technique developed during the test series. Also, the rate of unloading/reloading affected the calculated results because the crushed salt was always creeping. Additional data would improve our confidence in the experimental relationships developed.
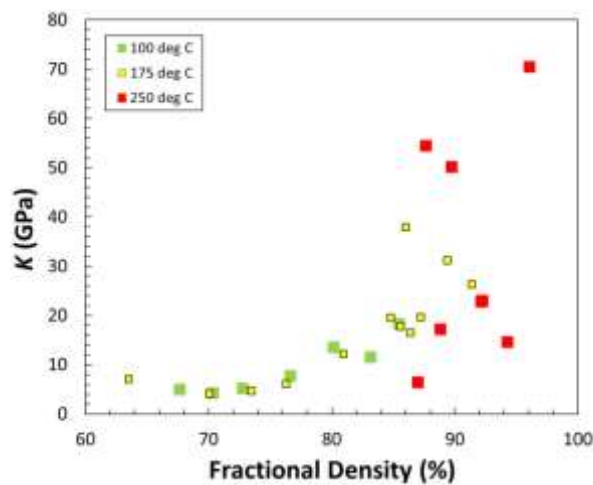

Figure 9. Fractional density versus bulk modulus, K.

3.2   Multistage Hydrostatic and Shear (Quasistatic and Creep) Tests

In this section examples of data from multistage tests are presented. After application of hydrostatic confining pressure, axial stress was increased in a quasistatic manner (slowly). Axial and radial displacement measurements were measured for each specimen as a function of time. This allowed axial, lateral, and volume strain to be determined. Figure 10 shows a lateral strain versus hydrostatic confining pressure record from a 250˚C test. As confining pressure increases, the crushed salt compacts. In all tests,

pressure was held constant for a brief time while preparing to apply axial force. This resulted in a small amount of isostatic creep compaction, about 1% in this test.
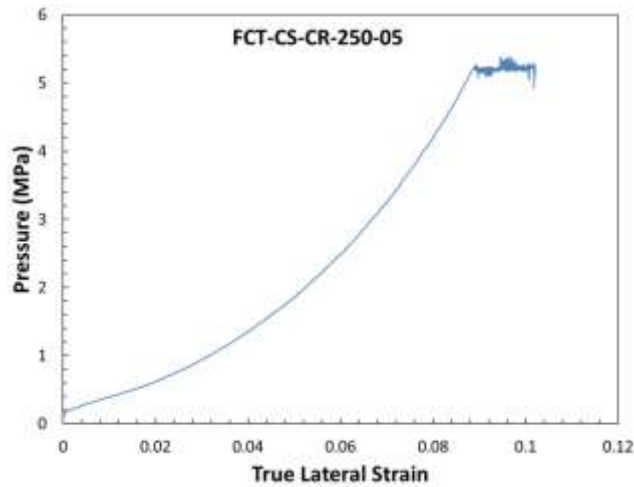

Figure 10. True lateral strain versus hydrostatic pressure.

In Figure 11, the detailed stress-strain response for the differential stress portion of this 250°C test is presented. During the initial axial loading, unload/reload loops are evident; as indicated, elastic moduli and Poisson's ratio are deduced from the axial and lateral strains measured during this portion of the test. This is accomplished through fitting of the unload/reload loops with a best fit line. The zoom view provides insight into data quality, quantity, and fidelity. Upon reaching the creep stress, stress levels are held constant. True strains as opposed to engineering strains are used due to the large deformations.
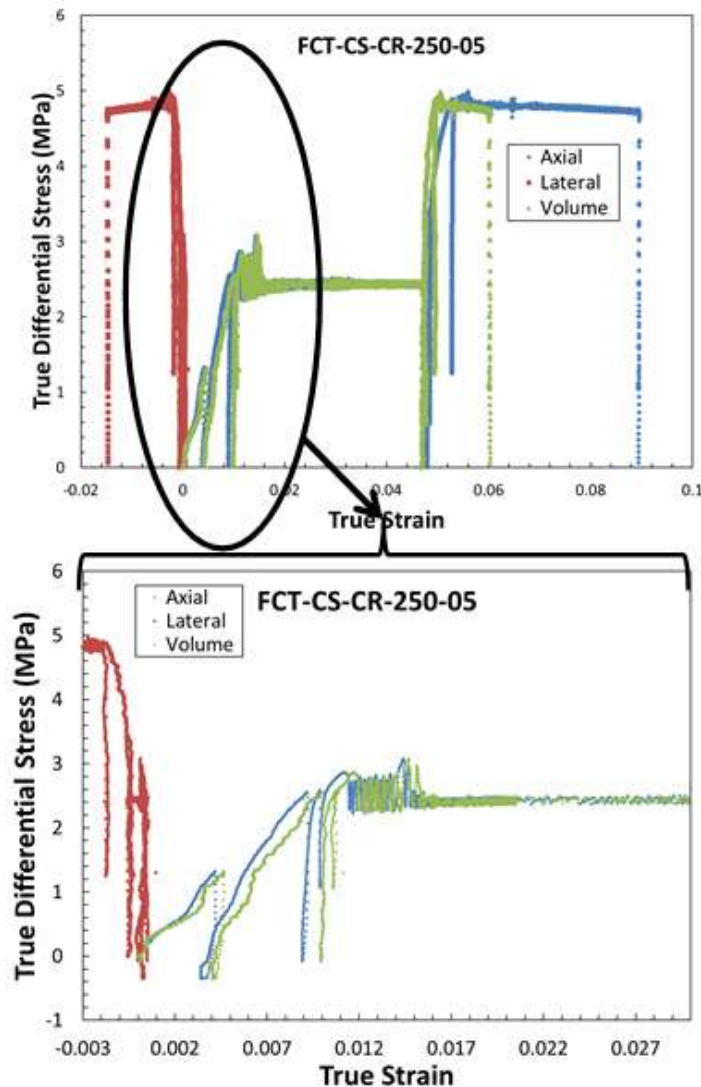
Figure 11. Stress-strain response for a typical 250°C test.

Figure 12 presents a comparison of true strain (axial, lateral, and volume) for the three test temperatures. The strain-time response elucidates the temperature effect upon compaction in shear deformation, since the confining pressure (2.5 MPa) and differential stresses (2.5, 5.0 MPa) are the same for each temperature. The 100°C test ran for about five and a half days and is missing some early data due to a data logger malfunction, the 175°C test ran for fourteen hours, and the 250°C test ran for about five hours. The fractional density at the start of the shear portion of the test increased with increasing test temperature due to a greater amount of volume strain during the hydrostatic portion of the test. And, although the starting fractional density is greatest for the 250°C sample, it experiences the greatest axial and lateral strain at these differential stresses, the strains for the 175°C are intermediate, and the 100°C sample experiences the smallest strains. The opposite trend is observed for volume strain. It is hypothesized this is due to greater compaction during the hydrostatic portion of the test resulting in greater lateral strain during the shear portion of the test, the higher the test temperature the less volume strain observed during the shear portion of the test.
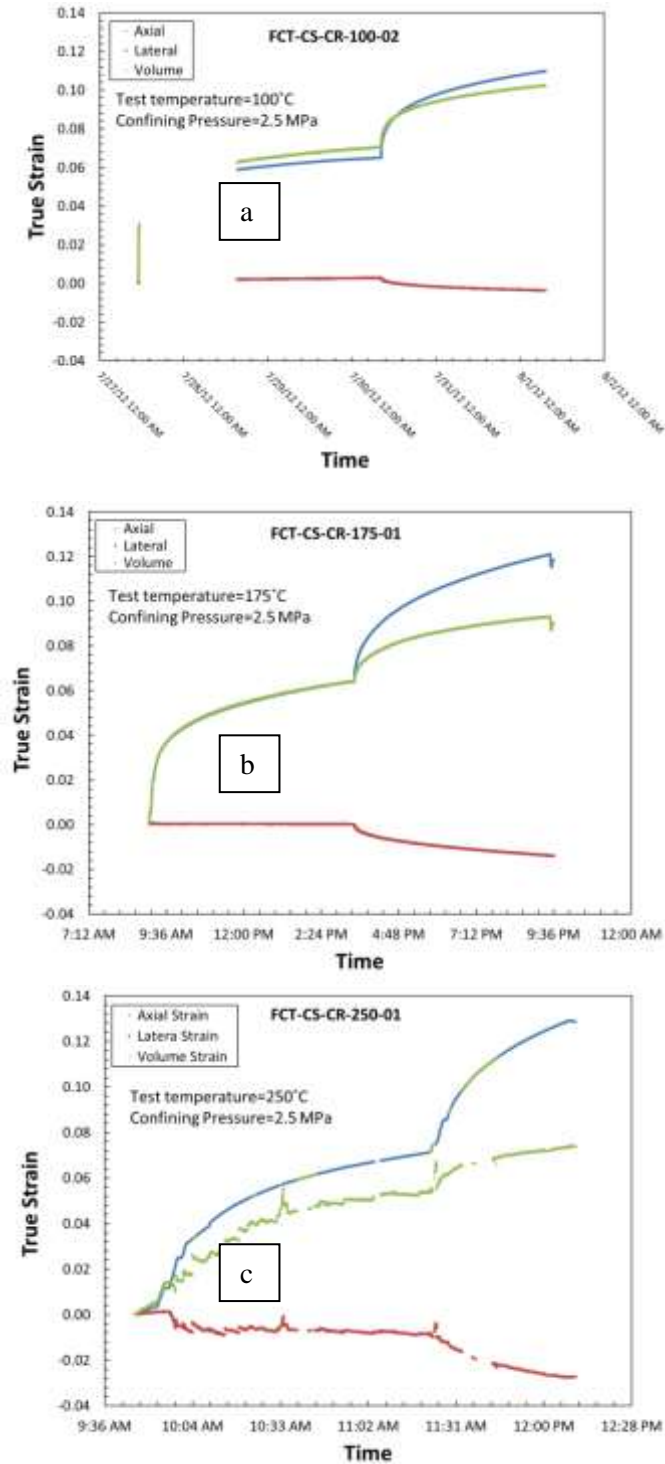
Figure 12. True strain versus time (a) 100˚C, (b) 175˚C, and (c) 250˚C.

The unload/reload loops during shear tests are used to determine Young's modulus during the deformation. In Figure 13, normalized Young's modulus is plotted against the fractional density. Young's modulus appears to increase consistently with increasing fractional density at a given temperature. Also, the data suggest Young's modulus decreases with increasing temperature; however, the data are too sparse to make definitive statements about the empirical relationships presented. The unload/reload loops

were dependent on unload and reload rates because the porous salt aggregate was always creeping; the combination of experimental technique and ongoing deformation gave rise to the data scatter observed. Young's modulus was normalized based on experimental data for intact WIPP salt (Brodsky, et al. 1996). For shear tests with higher confining pressures, Young's modulus increases. The specific values of Young's modulus used for the normalization process were 21, 27, and 43 GPa for confining pressures of 2.5, 5, and 10 MPa respectively.
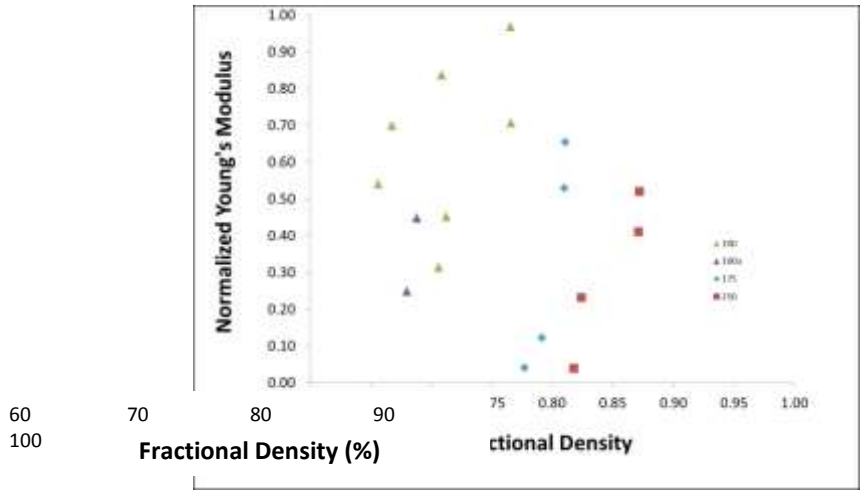

Figure 13. Fractional density versus normalized Young's modulus.

4.   CONSOLIDATION MECHANISMS

After the samples were successfully consolidated in the laboratory experiments, they were cut in half length-wise using a low-damage diamond wire saw and subsequently quartered. A variety of subsamples were prepared for observational work. The quarter-round subsections were broken by hand to expose a surface of the compacted material, which was sputter-coated and examined by SEM. The quarter-round pieces were used to prepare for optical sections and thick-thin sections. A unique technique was successfully attempted here for the first time, which involved plucking single grains from the consolidated mass, and then cleaving, etching and examining them.

Consolidation processes at high porosity involve instantaneous grain rearrangement and microfracture. These processes remove void space to a point at which grain boundary processes and crystal plastic mechanisms begin to dominate further porosity reduction. As porosity is reduced, plastic deformation proceeds, which with attendant and immediate increase in dislocation density is accommodated by slip along the dodecahedral {110} planes. Presented are a few photomicrographs from tests that were taken to <10% porosity.

Extraordinary crystal deformation is shown in Figure 14. This image is taken in transmitted light on a thick-thin section prepared from granular salt reconsolidated to low porosity at 250˚C. Exceptional crystal plasticity and compatible grain boundaries are exhibited between the elongate grains in the center of the frame. Contrast the plentiful fluid inclusions in the relatively large equant grains in the lower left and upper right quadrants of the field of view with the absence of fluid inclusions in the paired grains that display the tight boundary and exceptional elongation. Under these conditions at low porosity the densification processes involve plasticity coupled pressure solution (Spiers and Brzesowsky, 1993).

Also portrayed in the photomicrograph in Figure 14 are the pulverized grains clustered on the left lower area of view. All similar minute grains have been completely consumed between the two elongate grains. Elongation facilitated by slip on {110} planes apparently has moved nearly all the internal fluid inclusions to the grain boundaries. The fluid thereby made available to the grain-boundary was sufficient for pressure solution and consumption of the fine grains.
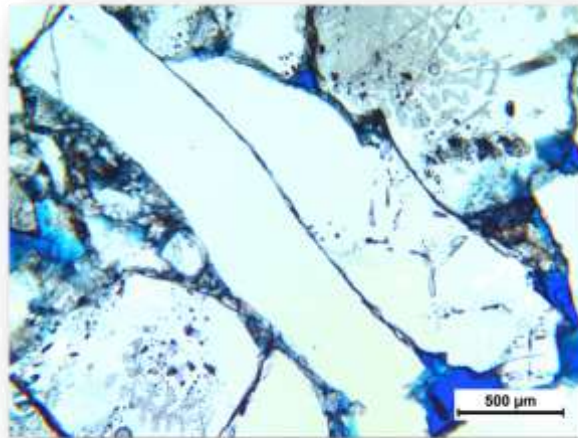

Figure 14. Extensive Grain Deformation During Reconsolidation at 250˚C.

A similarly striking photomicrograph is shown in Figure 15, in which the motion of internal fluid inclusions is captured on {110} planes and very tightly closed grain boundaries. Magnification is the same as the micrograph above and the blue hue is caused by epoxy impregnation. Fluid inclusions tend to collect along the tight grain boundaries, as might be expected as the fluid itself promotes creation of the

grain boundary. The abundance of fluid inclusions typical of Permian bedded salt and their undisturbed cubic habit are shown at a greater magnification in the inset photograph. The high degree of mobility of the inclusions can be seen in the dark images at an angle to the grain boundaries (presumably along {110}).
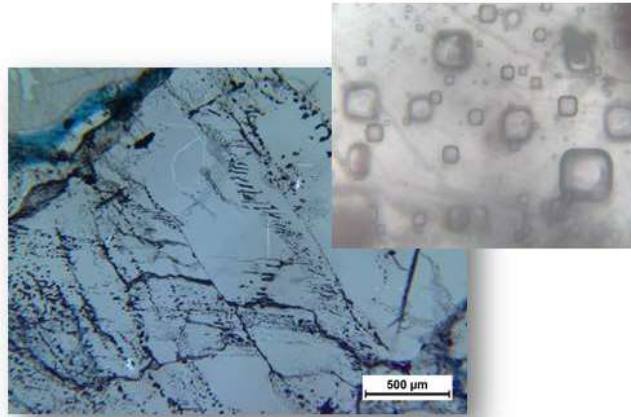

Figure 15. Glide of Fluid Inclusions Along Slip Planes 250°C.

The photomicrograph in Figure 16 is taken from a single grain extricated from FCT-CS-SQ-250-01 (see Table 2), which was consolidated at 250°C to measured volumetric strains of 31%. Highly distorted grains, such as these, were cleaved with some difficulty. One first notices that the cleavage plane itself is highly warped and gives the surface an undulatory fabric. To highlight the substructure, the cleaved chip was etched in methanol saturated with $PbCl_2$ and stopped in butanol. The crystal structure exhibits arrays of well-developed subgrains indicative of thermally activated climb recovery. In addition, the free-dislocation density within the polygons is very low, also indicating recovery by climb.
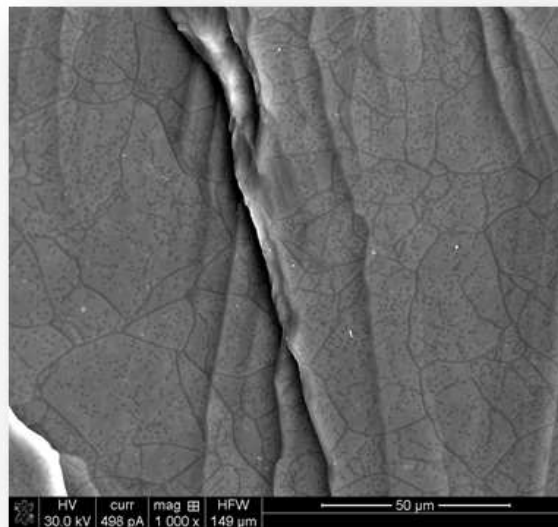

Figure 16. Etched Cleavage Chips from Samples Consolidated at 250°C.

Microscopic studies will be continued to elucidate salt substructure features at each temperature.

5. CONCLUSIONS

An experimental program was implemented to systematically perform a qualitative evaluation of crushed salt consolidation as a function of stress and temperature conditions. The laboratory studies provide consolidation behavior for temperatures to 250˚C and stresses to 20 MPa.

The test matrix includes isostatic, shear, and creep tests in order to determine elastic properties as a function of temperature and fractional density. Determinations of elastic properties versus fractional density have been made, however the limited data constrains investigation of these relationships. The experimental test conditions of temperature, pressure, and shear were applied to acquire data for use in fitting constitutive models with a minimum number of tests, while still exploring the full range of desired temperature, pressure and stress space.

An important observation during these tests is production of brine from the pore pressure port for 250˚C tests during the heating phase when the specimen was unconfined. This observation suggests the existence of some amount of trapped brine (i.e., intragranular porosity) and has implications for assumptions of a dry environment for high level waste disposal in bedded salt.

6.   REFERENCES

1.   Aubertin, M. and H.R. Hardy. 1996. The Mechanical Behavior of Salt, Proceedings of the Fourth Conference. Montreal Canada. Trans Tech Publications. ISBN 0-87849-103-1.

2.   Brodsky, N.S., F.D. Hansen, and T.W. Pfeifle. 1996. Properties of Dynamically Compacted WIPP Salt. Proceeding of the 4th Conference on the Mechanical Behavior of Salt, Trans Tech Publications, Clausthal-Zellerfeld, Germany. SAND96-0838C.

3.   Callahan, G.D. 1999, Crushed Salt Constitutive Model, SAND98-2680. Sandia National Laboratories, Albuquerque, NM.

4.   Hansen, F.D. and C.D. Leigh. 2011. Salt Disposal of Heat-generating Nuclear Waste, SAND2011-0161. Sandia National Laboratories, Albuquerque, NM.

5.   Spiers, C.J. and R.H. Brzesowsky. 1993. Densification Behaviour of Wet Granular Salt: Theory versus Experiment. 7th Symposium on Salt. Vol. I. Elsevier Science Publishers B.V. Amsterdam.

6.   Wallner, M., K-H Lux, W. Minkley, and H.R. Hardy. 2007. The Mechanical Behavior of Salt, Proceeding of the Sixth Conference. Hannover Germany. Balkema. ISBN 13: 978-415-444398-2.